Inorg. Chem. **2008**, *47*, 2464−2471

Modulated Misfit Structure of the Thermoelectric $[Bi_{0.84}CaO_2]_2[CoO_2]_{1.69}$ Cobalt Oxide

Hervé Muguerra,[†] Dominique Grebille,*[,†] Emmanuel Guilmeau,[†] and Rudi Cloots[‡]

Laboratoire CRISMAT (UMR CNRS 6508), ENSICAEN, 6 Bd Maréchal Juin, 14050 Caen Cedex, France, and Laboratory of Structural Inorganic Chemistry, Chemistry Department B6, University of Liège, Sart-Tilman, B4000 Liège, Belgium

Received August 31, 2007

The structure of the thermoelectric lamellar misfit cobalt oxide $[Bi_{0.84}CaO_2]_2[CoO_2]_{1.69}$ has been refined using single crystal X-ray diffraction data. Using the four dimensional superspace formalism for aperiodic structures, the superspace group is confirmed $P2/m(0\delta1/2)$ ($a_1 = 4.9069(4)$, $b_1 = 4.7135(7)$, $b_2 = 2.8256(4)$, $c_1 = 14.668(5)$ Å, $\beta_1 = 93.32(1)°$). The modulated displacements and site occupancies have been refined and are both compatible with the misfit character of the structure, and with a longitudinal modulation of the Bi−O layers of the structure. This modulation is similar to the corresponding one in the related Sr phase $[Bi_{0.87}SrO_2]_2[CoO_2]_{1.82}$, but now oriented in the orthogonal direction. Because its incommensurate wavelength is locked with the aperiodicity of the misfit structure, it is possible to distinguish between the modulation parameters induced by the accommodation of both subsystems and those related to the longitudinal modulation of the Bi−O layers. In this original structure, two independent aperiodic phenomena coexist in an single crystallographic direction. A particular attention has been paid to the structural configuration of the CoO_2 layer, in relation with other similar phases. The thermoelectric properties are probably directly related to the specific distortion of the compressed layer, but the different measured values for the Seebeck coefficient cannot be related to a significant modification of the CoO_6 octahedra.

1. Introduction

3d transition metal oxides are well-known for their ability to form mixed valence compounds, associated to nonstoichiometry, involving very specific electronic properties. Dealing for example with superconducting copper oxides, the nonstoichiometry is related to a partial occupation of the oxygen sites.[1] In the case of some Mn oxides, large magnetoresistance is associated to appropriate partial substitutions of divalent or trivalent cations, giving rise to electron density localization and charge and orbital ordering.[2] The present study is devoted to thermoelectric cobalt oxides. An original way to obtain nonstoichiometry and mixed valence in these cobalt oxides is to build the so-called misfit layered structures. Such structures involve two crystal subsystems, which share two unit cell basic vectors, but show incommensurate periodicities along the third direction.[3,4] The most interesting property associated to this type of cobalt oxides is a high thermoelectric power[5,6] which is characterized by a large Seebeck coefficient S (typically 100–150 μV/K). This property is associated to the systematic presence of pseudohexagonal layers of edge-sharing CoO_6 octahedra building a CdI_2 type slab. Between these layers, various rocksalt type blocks can be intercalated, which can differ either by the number of constitutive unique layers, or by the chemical species involved in these layers. The first famous thermoelectric oxide Na_xCoO_2[5] is characterized by only one partially occupied Na hexagonal plane. According to the x values ($0.3 \leq x \leq 1$), the electron doping of the CoO_2 layer and the corresponding Co valence can be continuously modified. Another well-known compound is the so-called

* To whom correspondence should be addressed. E-mail: dominique.grebille@ensicaen.fr. Tel.: +33 2452611. Fax: +33 2951600.
† Laboratoire CRISMAT (UMR CNRS 6508).
‡ University of Liège.

(1) Raveau, B. *Crystal Chemistry of High T_c Superconducting Copper Oxides*; Springer-Verlag: New York, 1991.
(2) Rao, C. R.; Raveau, B. *Colossal Magnetoresistance, Charge Ordering and Related Properties of Manganese Oxides*; World Scientific: Hackensack, NJ, 1998.
(3) Miyazaki, Y. *Solid State Ion.* **2004**, *172*, 463.
(4) Hervieu, M.; Michel, C. *C. R. Chimie* **2007**, *10*, 604.
(5) Terasaki, I.; Sasago, Y.; Uchinokura, K. *Phys. Rev. B* **1997**, *56*, R12685.
(6) Li, S.; Funahashi, R.; Matsubara, I.; Ueno, K. *J. Mat. Chem.* **1999**, *9*, 1659.

10.1021/ic701717f CCC: $40.75
Published on Web 03/04/2008

"$Ca_3Co_4O_9$" compound[7] (CCO), with also very promising thermoelectric properties ($S \approx 120\ \mu$V/K). In this misfit structure, a three layers rocksalt block (Ca−O, O−Co, Ca−O) are present.[8,9] Another series is obtained with four layers in each rocksalt block: a central double BiO layer is sandwiched between AE−O layers where AE stands for alkaline earth species (Ca, Sr, Ba). These compounds exhibit large S values (around 150 μV/K for the AE = Ca). According to the corresponding atomic radii, one obtains different misfit ratios from 1.62 to 2, and a corresponding decrease of the Seebeck coefficient is observed;[10−12] so that, the Ca compound, with a misfit ratio of 1.69, is still a valuable candidate for thermoelectric performance. This structural parameter is a first key to understand the corresponding correlation between nonstoichiometry and physical properties, but is not sufficient by itself. Further optimizations need also a deeper understanding of the influence of the nature, the structure and the disorders or modulations in the rocksalt block, on the electronic structure of the CoO_2 subsystem.

The corresponding compounds are rather complex due to their misfit character, which imposes the superspace formalism for the description of their aperiodic structures.[13] At least four different and rationally independent periodicities are simultaneously present in the crystal structure and this is the reason why one needs to build a 4D supercrystal. The real crystal can be properly described by a section of this supercrystal in the 3D physical space. Each subsystem is then characterized by its own 3D average cell (a_1, b_1, c_1, β_1 for the rocksalt system arbitrarily chosen as reference, and $a_2 = a_1$, $b_2 = b_1/\delta$, $c_2 = c_1$, $\beta_2 = \beta_1$ for the second CoO_2 system.). Atomic positions are then described as atomic modulated strings, characterized by displacive or occupational modulation functions. With this model, diffracted intensities can be calculated and refined taking into account simultaneously and coherently two basic main reflection sets, and pure satellite reflections resulting from the mutual modulation of the two systems. Among the four-layer compounds, only the structure of the $[Bi_{0.87}SrO_2]_2[CoO_2]_{1.82}$ phase (BSCO) was accurately studied,[14] which first confirmed the misfit incommensurate character and second, described the bonding scheme between the two subsystems. Moreover, an intrinsic incommensurate modulation mainly attached to the Bi−O layers was also observed and discussed. Independently from the misfit character of the structure, this modulation was evidenced by the observation of another set of satellite reflections and was defined still by another incommensurate periodicity, needing a 5D description.

More recently, the corresponding Ca phase (BCCO in the following) has been studied for its enhanced thermoelectric properties and for iodine intercalation capabilities.[15,16] It was expected to display the same type of structure as BSCO, with a smaller misfit ratio (1.69), but, due to the poor crystalline quality of the samples, only the crystal symmetry and a model of the average structure could be proposed.[16] Improving the synthesis conditions, we have been able to grow samples of good enough quality to proceed to a single crystal X-ray diffraction data collection and to finalize the structure refinement involving all possible modulated displacements related to the misfit character or still to the presence of Bi−O layers. It will appear that this compound presents an original structure which was not directly predictable as isotypic to the BSCO one. This new structure allows us to proceed to a more detailed comparison of the different CoO_2 layers of all these various phases.

2. Experimental Details

Single crystals were grown by the flux method. Precursor powders of Bi_2O_3, $CaCO_3$, and Co_3O_4 were mixed with a cationic composition of Bi:Ca:Co = 2.5:2.5:2 and calcined at 850 °C for 50 h. The resulting powder was mixed and calcined again in the same conditions. The powder was then mixed with Bi_2O_3, K_2CO_3, and KCl powder (weight ratio of 3:10:70:17) and heated in an alumina crucible at 900 °C for 20 h. The temperature was cooled down to 700 °C with a rate of 2 °C/h and next furnace-cooled. The platelike single crystals have a typical hexagonal surface area of 5–10 mm^2 for a thickness of 10–20 μm.

An elemental analysis was performed using energy dispersive spectroscopy and gave the cationic ratio Bi:Ca:Co = 1.84(5):2.00:1.62(5). Oxygen titrations were not possible with a sufficient accuracy according to the small mass of the analyzed samples.

The single crystal X-ray diffraction study was performed at room temperature using Mo Kα radiation with a Bruker Kappa CCD diffractometer. A first cell was determined using reflections with $\theta < 30°$ and is compatible with the monoclinic system: $a_1 = 4.9069(4)$, $b_1 = 4.7135(7)$, $c_1 = 29.337(5)$ Å, $\beta_1 = 93.32(1)°$. Other reflections with high intensities were not predicted by this cell, but could be indexed, using a new b_2 parameter, corresponding to the expected misfit structure. A new cell could be refined: $a_2 = a_1$, $b_2 = 2.8256(4)$ Å, $c_2 = c_1$, and $\beta_2 = \beta_1$. The modulation vector $\mathbf{b}_2^* + \mathbf{c}^*$ was then introduced in order to index all the observed reflections (Figure 1). We can emphasize here that even if the quality of the present crystal is better than the first one used for the crystal symmetry study,[16] a rather large mosaïcity is still observed. Data collection was performed using $\varphi-\omega$ scans with $0 < \theta < 45°$, with steps of 0.3°/frame and a sample–detector distance of 34 mm. Data reduction and integration was performed using the EVALCCD software[17] in different steps: main reflections compatible with the first cell (a_1, b_1, c_1, β_1), then with the second one (a_2, b_2, c_2, β_2), and finally, first

(7) Masset, A. C.; Michel, C.; Maignan, A.; Hervieu, M.; Toulemonde, O.; Studer, F.; Raveau, B.; Hejtmanek, J. *Phys. Rev. B* **2000**, *62*, 166.
(8) Grebille, D.; Lambert, S.; Bourée, F.; Petíček, V. *J. Appl. Crystallogr.* **2004**, *37*, 823.
(9) Ling, C. D.; Aivazian, K.; Schmid, S.; Jensen, P. *J. Solid State Chem.* **2007**, *180*, 1446.
(10) Maignan, A.; Hébert, S.; Hervieu, M.; Michel, C.; Pelloquin, D.; Khomskii, D. *J. Phys.: Condens. Matt.* **2003**, *15*, 2711.
(11) Funahashi, R.; Matsubara, I.; Sodeoka, S. *Appl. Phys. Lett.* **2000**, *76*, 2385.
(12) Hervieu, M.; Maignan, A.; Michel, C.; Hardy, V.; Créon, N.; Raveau, B. *Phys. Rev. B* **2003**, *67*, 045112.
(13) Janssen, T.; Janner, A.; Looijenga, A.; de Wolff, P. M. *International Tables for Crystallography*; Kluwer Academic Publishers: Dordrecht, 1992; Vol. *C*, p 797.
(14) Leligny, H.; Grebille, D.; Pérez, O.; Masset, A. C.; Hervieu, M.; Raveau, B. *Acta Cryst. B* **2000**, *56*, 173.
(15) Guilmeau, E.; Pollet, M.; Grebille, D.; Hervieu, M.; Muguerra, H.; Cloots, R; Mikami, M.; Funahashi, R. *Inorg. Chem.* **2007**, *46*, 2124.
(16) Grebille, D.; Muguerra, H.; Pérez, O.; Guilmeau, E.; Rousselière, H.; Funahashi, R. *Acta Cryst. B* **2007**, *63*, 373.
(17) Duisenberg, A. J. M.; Kroon-Batenburg, L. M. J.; Schreurs, A. *J. Appl. Crystallogr.* **2003**, *36*, 220.

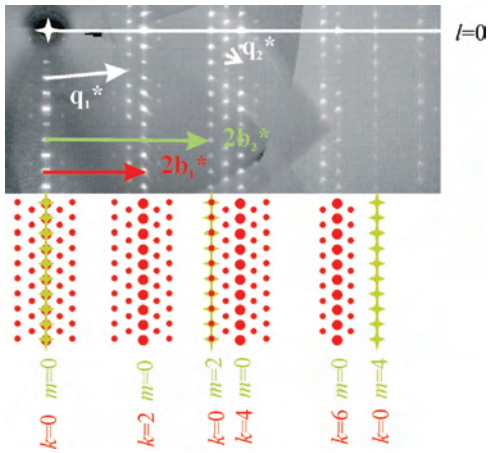

Figure 1. Reconstructed (0*kl*) reciprocal plane: [large (respectively small) red circles] main (respectively satellite) reflections of the first sublattice ($\mathbf{b}_1^*$ and $\mathbf{q}_2^*$); [crosses] main reflections of the second subsystem ($\mathbf{b}_2^*$).

Table 1. Crystal Data and Structure Refinement Results

chemical formula	$[Bi_{0.84}CaO_2]_2[Co_{0.96}O_2]_{1.69}$
crystal size (μm)	≈300 × 300 × 30
crystal system	monoclinic
cell parameters	
a_1 (Å)	4.9069(4)
b_1 (Å)	4.7135(7)
c_1 (Å)	29.337(5)
β (deg)	93.32(1)
V (Å^3)	338.682(6)
$\mathbf{q}^* = \delta\mathbf{b}^* + \mathbf{c}^*/2$	$\delta = 1.6907(2)$
superspace group	$P2/m(0\delta\frac{1}{2})s0$
Z	2
formula weight	511.43
ρ (g/cm^3); μ (1/cm)	7.007; 608.6
wavelength (Å)	0.71073
T (K)	300
θ_{max} (deg); $(\sin\theta/\lambda)_{max}$	45; 0.995
internal consistency factor R_{int} (after absorption correction)	2.90
measured/observed reflections	11521/8421
transmission factors	
T_{min}; T_{max}	0.0047; 0.2416
number of parameters actually refined	112
weighting scheme	$1/\sigma^2$
$\Delta\rho_{min}$ (e$^-$/Å^3)	−7.07
$\Delta\rho_{max}$ (e$^-$/Å^3)	6.71
number of unique reflections (with $I \geq 3\sigma(I)$)	4230
corresponding reliability factor R/wR (%)	5.02/4.20
main reflections	2912
corresponding reliability factor R/wR (%)	4.32/3.91
1st order satellite refined	1225
corresponding reliability factor R/wR (%)	7.55/6.28
2nd order satellite refined	93
factor R/wR (%)	23.24/22.40
1st subsystem	1638
factor R/wR (%)	4.03/3.59
2nd subsystem	887
factor R/wR (%)	5.38/4.47
common reflections	387
factor R/wR (%)	3.80/4.11

and second order satellite reflections of the first lattice. These data were corrected for Lorentz-polarization and absorption, using the morphology of the crystal. Then, they were rescaled using common reflections, merged and averaged using the JANA2000 software.[18] Crystal data are summarized in Table 1.

(18) Petříček, V.; Dušek, M.; Palatinus, L. *Jana2000. The crystallographic computing system*; Institute of Physics: Praha, Czech Republic, 2000.

3. Structure Refinement

A first analysis of the crystal symmetry of BCCO has been given using reconstructed reciprocal planes.[16] The (*hk*0) or (0*kl*) planes clearly show the usual features associated with similar misfit structures, i.e. the superposition of two lattices of main reflections involving common a and c parameters (4.9069(4) and 29.337(5) Å), but different b_1 and b_2 parameters (4.7135(7) and 2.8256(4) Å, $\delta = b_1/b_2 = 1.691(1)$). This aperiodic ratio is currently observed in misfit cobalt lamellar oxides involving Ca in the rocksalt system 1. Extra weak reflections are also involved, which can be indexed using simultaneously both $\mathbf{b}_1^*$ and $\mathbf{b}_2^*$ reciprocal basic vectors: they are pure satellite reflections of the aperiodic structure and need four indices h, k, l and m, with k and m not equal to 0, to define the corresponding scattering vector (Figure 1):

$$S = ha_1^* + kb_1^* + lc_1^* + mq_1^*$$

with $\mathbf{q}_1^* = \mathbf{b}_2^* + \mathbf{c}_1^* = \delta\mathbf{b}_1^* + \mathbf{c}_1^*$.

The (0*kl*) plane shown in Figure 1 is characterized by a pseudo reflection condition $k = 2n$ which is not fulfilled in other planes like (2*kl*) for example, so that the global diffraction pattern is primitive with a pseudo C centering. The sublattice 1 is also characterized by a systematic reflection condition $l = 2n$, so that it can be described in a half-primitive cell with a half c parameter and in the superspace Laue class $P2/m(0\delta1/2)$.[16]

The intensity distribution of the satellite reflections is quite different from the corresponding one of the related Sr phase $[Bi_{0.87}SrO_2]_2[CoO_2]_{1.82}$.[14] In the latter one, the misfit character was clearly observable in the (0*kl*) reciprocal plane, but the (*h*0*l*) plane was characterized by a modulation scheme with a specific modulation vector, independent from the previous aperiodicity. We can recognize now in the (0*kl*) reciprocal plane of the present Ca compound both specific features of the Sr phase (Figure 1): reflections of higher intensities define the two main sublattices of a misfit structure, but satellites are distributed around the main reflections of the first sublattice in a similar manner as in the (*h*0*l*) plane of the Sr phase. A specific modulation, partly independent from the misfit structure, can then be assumed for the first sublattice, with a modulation vector $\mathbf{q}_2^* = \varepsilon\mathbf{b}_1^* - \mathbf{c}_1^*$ with $\varepsilon = 0.309$. From this value, we can see that $\mathbf{q}_2^* = (2-\delta)\mathbf{b}_1^* - \mathbf{c}_1^* = 2\mathbf{b}_1^* - \mathbf{q}_1^*$, so that a satellite reflection $h\mathbf{a}^* + k\mathbf{b}_1^* + l\mathbf{c}_1^* + m_2\mathbf{q}_2^*$ for this modulated scheme can also be expressed as $h\mathbf{a}^* + (k + 2m_2)\mathbf{b}_1^* + l\mathbf{c}_1^* - m_2\mathbf{q}_1^*$ in the same general indexation used for the misfit structure. The two aperiodicities are locked together. It is the reason why, in the present case, only four indices and not five, are sufficient for the complete indexation of the diffraction pattern. A five dimensional description is not necessary here, and the structure refinement can be developed in a four dimensional approach using the superspace formalism.[13] The corresponding modulation functions are assumed to account for both aspects of the present unique aperiodicity. This will be discussed further.

A preliminary model was introduced according to the expected average misfit structure.[16] Neutralizing the rational

Table 2. Structural Refined Parameters[a]

atom	wave	occupancy	*x*	*y*	*z*	U_{iso} or U_{eq}
			1st Subsystem			
Ca1		1	0.6924(1)	0[c]	0.09890(3)	0.0119(2)
	s,1		−0.0168(3)	0[b]	−0.00140(6)	
	c,1		0[b]	0[c]	0[b]	
Ca2		1	0.1937(1)	0.5[c]	0.09889(3)	0.0119(2)
	s,1		0.0164(3)	0[b]	−0.00093(6)	
	c,1		0[b]	−0.0053(4)	0[b]	
Oa1		1	0.6885(4)	0.5[c]	0.1218(1)	0.0138(4)
	s,1		0.006(1)	0[b]	−0.0015(2)	
	c,1		0[b]	0[c]	0[b]	
Oa2		1	0.2173(4)	0[c]	0.1221;(1)	0.0134(4)
	s,1		−0.005(1)	0[b]	0[c]	
	c,1		0[b]	0[c]	0[b]	
Bi1		0.834(2)	0.7417(1)	0.5[c]	0.192242(8)	0.0220(2)
	s,1	−0.174(2)	0.0086(2)	0[b]	−0.00080(2)	
	c,1	0[b]	0[b]	−0.0263(3)	0[b]	
	s,2	0[b]	0[b]	−0.0003(6)	0[b]	
	c,2	0.231(9)	−0.0071(3)	0[b]	0.00025(3)	
Bi2		0.845(2)	0.21644(5)	0[c]	0.192278(7)	0.0196(2)
	s,1	−0.136(2)	−0.0071(2)	0[b]	−0.00055(2)	
	c,1	0[b]	0[b]	−0.0356(3)	0[b]	
	s,2	0[b]	0[b]	−0.0116(6)	0[b]	
	c,2	−0.141(9)	0.0021(2)	0[b]	0	
Ob1		1	0.7802(5)	0[c]	0.18490(12)	0.0187(7)
	s,1		−0.008(2)	0[b]	−0.0020(2)	
	c,1		0[b]	0.014(2)	0[b]	
	s,2		0[b]	0.016(3)	0[b]	
	c,2		0.008(3)	0[b]	0.0025(5)	
Ob2		1	0.1703(5)	0.5[c]	0.1847(2)	0.0192(7)
	s,1		0.008(2)	0[b]	0[c]	
	c,1		0[b]	0.006(2)	0[b]	
	s,2		[b]	−0.018(3)	0[b]	
	c,2		0.007(3)	0[b]	−0.0027(5)	
			2nd Subsystem			
Co		0.965(3)	0.25001(5)	0.25[c]	−0.00004(1)	0.00489(6)
	s,1		0[b]	0[c]	0[b]	
	c,1		−0.0038(2)	0[b]	0.00167(3)	
	s,2		0[b]	0[c]	0[b]	
	c,2		0[c]	0[b]	−0.00119(3)	
O1		1	0.5698(3)	0.25[c]	−0.03415(5)	0.0075(3)
	s,1		0[b]	0.002(2)	0[b]	
	c,1		−0.0055(6)	0[b]	0.0014(2)	
	s,2		0[b]	0.013(2)	0[b]	
	c,2		0[c]	0[b]	0[c]	
O2		1	−0.0698(3)	0.25[c]	0.03427(6)	0.0070(3)
	s,1		0[b]	0[c]	0[b]	
	c,1		−0.0055(6)	0[b]	0.0015(2)	
	s,2		0[b]	0[c]	0[b]	
	c,2		0[c]	0[b]	−0.0030(2)	

[a] The designation s,*i* (respectively c,*i*) correspond to the *i*th order of the sine (respectively cosine) components of the Fourier series of the modulation function. [b] Fixed to zero by symmetry. [c] Fixed to zero because it is not significant.

part of the modulation vector by the appropriate 4D centering (0, 0, 1/2, 1/2), the equivalent superspace group $X2/m(0\delta0)$ was considered with the **W** matrix relating the two subsystems.

$$\begin{pmatrix} 1 & 0 & 0 & 0 \\ 0 & 0 & 0 & 1 \\ 0 & 0 & 1 & 0 \\ 0 & 1 & 0 & 0 \end{pmatrix}$$

Considering the primitive character of the cell, two independent Bi atoms and two independent O atoms (respectively two Ca atoms and two O atoms) were introduced for the BiO layer (respectively for the CaO layer). Then, displacive modulation functions were introduced for all atoms up to the second order, and occupation modulation functions for Bi in the BiO layers, where they appear to be significant. Average occupancies of other sites were refined, but only the Bi and Co sites gave significantly reduced values. According to our previous symmetry analysis, two hypotheses should be considered: $P2/m(0\delta1/2)00$ and $P2/m(0\delta1/2)s0$. The diffraction pattern in relation with the reflection conditions is not sufficient to make a choice. The structure was refined in both cases and the results were slightly better in the second case. Anywhere, when comparing the structural results, very similar positions and modulations are obtained, and the differences are not clearly significant, so that the description will be developed only with the $P2/m(0\delta1/2)s0$ spacegroup. Agreement factors and structural parameters are summarized in Tables 1 and 2. A schematic representation of the misfit structure is given in Figures 2 and 3.

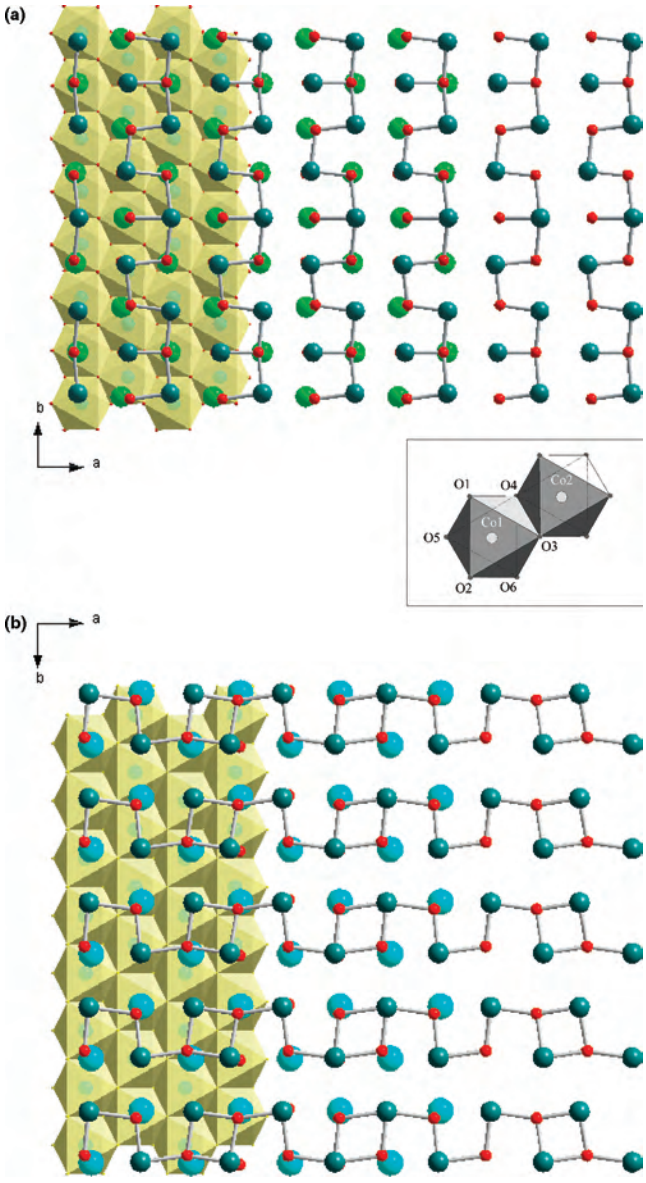

Figure 2. Schematic representation of the BCCO (a) and BSCO (b) structures projected along **c**: (dark blue circles) Bi; (green circles) Ca; (light blue circles) Sr; (small red circles) O. (a inset) Numbering of the Co and O atoms of the CoO_2 layers for the listing of interatomic distances and angles.

Based on the irrational ratio 1.69 between the two sublattices and to the refined partial average occupation parameters for Bi in subsystem 1 (0.84) and Co in subsystem 2 (0.965), the general derived chemical formula is $Bi_{1.68}Ca_2Co_{1.63}O_{7.38}$, compatible with the misfit formula $[Bi_{0.84}CaO_2]_2[Co_{0.97}O_2]_{1.69}$. The oxygen positions are here assumed to be totally occupied, but the refinement with X-ray data does not allow us to refine reliably such an occupation, so that oxygen vacancies are not excluded and could be then coupled with different values for the Co valence.

Relatively large residual maximal and minimal electronic densities are obtained, but these values are reached in the vicinity of the heavy Bi atoms, which are also heavily modulated and probably rather poorly simulated by two orders of harmonics for their displacive modulation parameters. These residuals represent around 1.5% of the corresponding electronic density around these atoms. They are

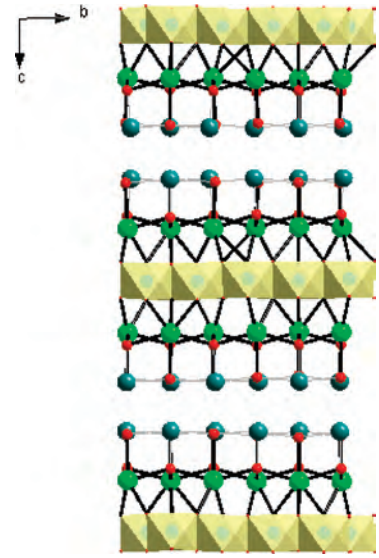

Figure 3. Schematic representation of the structure projected along **a**: (blue circles) Bi; (green circles) Ca; (small red circles) O; (black lines) CaO bonds.

quite equivalent to the corresponding ones obtained in the similar modulated chains in high T_c Bi based superconducting oxides. They must be related to the difficulties to find a proper model to describe both occupational and displacive modulations of these heavy atoms, which are probably also characterized by local disorders. The refined average occupation of the Bi site can also be biased by these difficulties and is slightly underestimated according to the EDS analysis.

4. Discussion

4.1. The CoO_2 Layer. The average structure of the CoO_2 layer is built with distorted edge-sharing CoO_6 octahedra distributed along a pseudohexagonal arrangement. The distortion mainly consists in a contraction of the slab along the stacking pseudoternary direction **c**. O−O interatomic distances can be grouped into long intralayer distances (2.80 Å) and very short interlayer ones (2.57–2.59 Å) (Table 3 and Figure 2). But this distortion does not modify the Co−O distances, which remain very close to each other (1.91Å) and very closed to equivalent distances in nondistorted CoO_6 octahedra (1.92 Å in Co_3O_4 for example). The contraction of the slab along **c** of about 8% with respect to a non distorted octahedra slab leads to a interlayer distance of 2.02 Å and is associated with a slight relative shift of the two O layers in the **a** direction of about 0.11 Å (elongation of about 4%). When considering the modulated displacements in this layer, the Co−O distances vary from 1.845 to 1.957 Å, but the bond-valence sum[19] remains constant (3.4). This modulated distortion is mainly due to the x component of the O displacement and will be explained further. The average internal distortion of the octahedra is probably an important key for the understanding of thermoelectric properties via the orbital energy splitting in this particular crystal field and symmetry. It is the reason why it is particularly interesting to compare the structural distortion in the related known

(19) Brese, N. E.; O'Keeffe, M. *Acta Cryst. B* **1991**, *47*, 192.

Table 3. Interatomic Distances and Angles for Different Structures of Layered Cobalt Oxides with CoO_2 Layers[a]

	BCCO	BSCO	CCO	CCO	$Na_{0.3}CoO_2$	$Na_{0.5}CoO_2$	$Na_{0.75}CoO_2$	$LiCoO_2$	$Na_xCoO_2.yH_2O$
reference	this study	14	8	9	21	22, 23	24, 25	26	27, 28
symmetry	*P2/m*	*I2/a*	*C2/m*	*C2/m*	*P6₃/mmc*	*Ccmm*	*P6₃/mmc*	*R$\bar{3}$m*	*P6₃/mmc*
S (μV/K)	150	120	120			95	95		
				Distances (Å)					
Co1−O5	1.913	1.917	1.894	1.903	1.891	1.914	1.911	1.921	1.855
Co1−O3	1.910	1.917	1.894	1.903	1.891	1.914	1.911	1.921	1.855
Co1−O1	1.907	1.907	1.904	1.909	1.891	1.903	1.911	1.921	1.855
Co1−O4	1.907	1.907	1.904	1.909	1.891	1.903	1.911	1.921	1.855
Co1−O2	1.907	1.907	1.904	1.909	1.891	1.903	1.911	1.921	1.855
Co1−O6	1.907	1.907	1.904	1.909	1.891	1.903	1.911	1.921	1.855
O1−O4	2.590	2.579	2.560	2.569	2.529	2.561	2.558	2.615	2.406
O1−O2	2.799	2.809	2.819	2.801	2.812	2.815	2.841	2.814	2.823
O1−O5	2.575	2.575	2.570	2.586	2.529	2.576	2.558	2.615	2.406
CO bond sum valence	3.42	3.40	3.49	3.43	3.58	3.43	3.39	3.30	3.95
valence from ref 29	3.20	3.20	3.35	3.28	3.49	3.22	3.18	3.02	4.00
valence from chemical formula	3.5	3.3	3.2[b]	3.2[b]	3.7	3.5	3.3	3.0	3.65
				Angles (deg)					
O2−O1−O3	60.26	60.20	59.73	59.72	60.00	60.01	60.00	60.00	60.00
O1−O3−O2	59.48	59.59	60.53	60.56	60.00	59.98	60.00	60.00	60.00
O3−O1−O4	56.50	56.67	57.14	57.37	56.22	57.01	56.28	57.45	54.08
O1−O3−O4	57.21	56.82	56.80	56.79	56.21	56.50	56.27	57.45	54.08
O1−Co1−O5	84.77	84.67	85.16	85.42	83.92	84.90	84.01	85.80	80.88
O1−Co1−O2	94.41	94.88	95.51	95.44	96.08	95.41	95.99	94.20	99.12
O1−Co1−O4	85.57	85.12	84.48	84.56	83.92	84.59	84.01	85.80	80.88
O4−Co1−O5	95.26	95.32	94.84	94.58	96.08	95.10	95.99	94.20	99.12
Co1−O3−Co2	95.35	95.32	94.84	94.58	96.08	95.10	95.99	94.20	99.12

[a] See Figure 2 for the atom numbering. [b] Average valence includes the Co sites in the two subsystems.

structures of other lamellar cobalt oxides. The structural parameters listed in Table 3 are very similar to each other for all the reported thermoelectric phases, and are only significantly different for the superconducting hydrated compound $Na_{0.35}CoO_2 \cdot yH_2O$.[20] Even with different crystal symmetries, and consequently with different constraints for the atomic positions, no real deviation is observed from the hexagonal pseudosymmetry of this layer. This structural configuration is particularly stable and this probably explains also the common stacking scheme between the two subsystems in this structural family.[16] Different methods have been used to estimate the Co valence, using either stereochemical parameters or electroneutrality considerations. According to the method, the results can be very different. Calculations using Brese and O'Keeffe[19] parameters are probably systematically overestimated, and the calculations based on the chemical formula are biased by the uncertainties about atomic vacancies. The more reliable method seems to be the interpolation method of Levasseur;[29,30] it gives very close values and cannot explain by itself the variations of thermoelectric power. Consequently, we must admit here that the significant differences of the thermoelectric power of these structures are probably related to electron charge transfer between the two subsystems and cannot be simply related to the structural configuration of the CoO_6 octahedra.

4.2. Rocksalt Subsystem. When looking first at the average atomic positions, one can notice a deviation of the *x* component of the atoms from the values 0.75 or 0.25 which would describe a homogeneous distribution of the atoms in the layer. The result is a well-known double chain configuration (along *y*) already often mentioned in the lamellar structures of Bi based high T_c superconducting oxides and related structures.[31–33] It is also met in the related Sr misfit cobalt oxide, but in this last case, the chains were aligned along *x*.

The larger modulated displacements (Table 3) concern on one hand the *x* component of the Ca atom and of the O atom of the CoO_2 layer and on the other hand, the *x* and *y* components of the Bi atom. The first contributions can be simply explained by stereochemical considerations: these

(20) Takada, K. *Nature* **2003**, *422*, 53.
(21) Lynn, J. W.; Huang, Q.; Brown, C. M.; Miller, V. L.; Foo, M. L.; Schaak, R. E.; Jones, C. Y.; Mackey, E. A.; Cava, R. J. *Phys. Rev. B* **2003**, *68*, 214516.
(22) Igarashi, D.; Miyazaki, Y.; Yubuta, K.; Kajitani, T. *Jpn. J. Appl. Phys.* **2007**, *46*, 304.
(23) Chen, X. Z.; Xu, Z. A.; Cao, G. H.; Shen, J. Q.; Qiu, L. M.; Gan, Z. H. *cond-ma* **2004**, 0412299.
(24) Huang, Q.; Khaybovitch, B.; Chou, F. C.; Cho, J. H.; Lynn, J. W.; Lee, Y. S. *Phys. Rev. B* **2004**, *70*, 134115.
(25) Lee, M.; Viciu, L.; Li, L.; Wang, Y.; Foo, M. L.; Watauchi, S.; Pascal Jr, R. A.; Cava, R. J.; Ong, N. P. *Nat. Mater.* **2006**, *5*, 537.
(26) Levasseur, S.; Ménétrier, M.; Suard, E.; Delmas, C. *Solid St. Ionics* **2000**, *128*, 11.
(27) Takada, K.; Sakurai, H.; Takayama-Muromachi, E.; Izumi, F.; Dilanian, R. A.; Sasaki, T. *Nature* **2003**, *422*, 53.
(28) Argyriuo, D. N.; Radaelli, P. G.; Milne, C. J.; Aliouane, N.; Chapon, L. C.; Chemseddine, A.; Veira, J.; Cox, S.; Mathur, N. D.; Midgley, P. A. *J. Phys.: Cond. Matter* **2005**, *17*, 3293.
(29) Levasseur, S. Contribution à l'étude des phase $Li_x(Co,M)O_2$ en tant que matériaux d'électrode positive des batteries Li-ion. Effets combinés de la surstoechiométrie en lithium et de la substitution (M = Ni, Mg). Ph.D. Thesis, ICMCB-Université Bordeaux 1, Talence Cedex, France, 2001.
(30) Pollet, M.; Doumerc, J. P.; Guilmeau, E.; Grebille, D.; Fagnard, J. F.; Cloots, R. *J. Appl. Phys.* **2007**, *101*, 083708.
(31) Grebille, D.; Leligny, H.; Ruyter, A.; Labbé, Ph.; Raveau, B. *Acta Cryst. B* **1996**, *52*, 628.
(32) Jakubowicz, N.; Grebille, D.; Leligny, H.; Evain, M. *J. Phys. (Paris)* **1999**, *11*, 3997.
(33) Pérez, O.; Leligny, H.; Grebille, D.; Grenêche, D.; Labbé, Ph.; Groult, D.; Raveau, D. *Phys. Rev. B* **1997**, *55*, 1236.

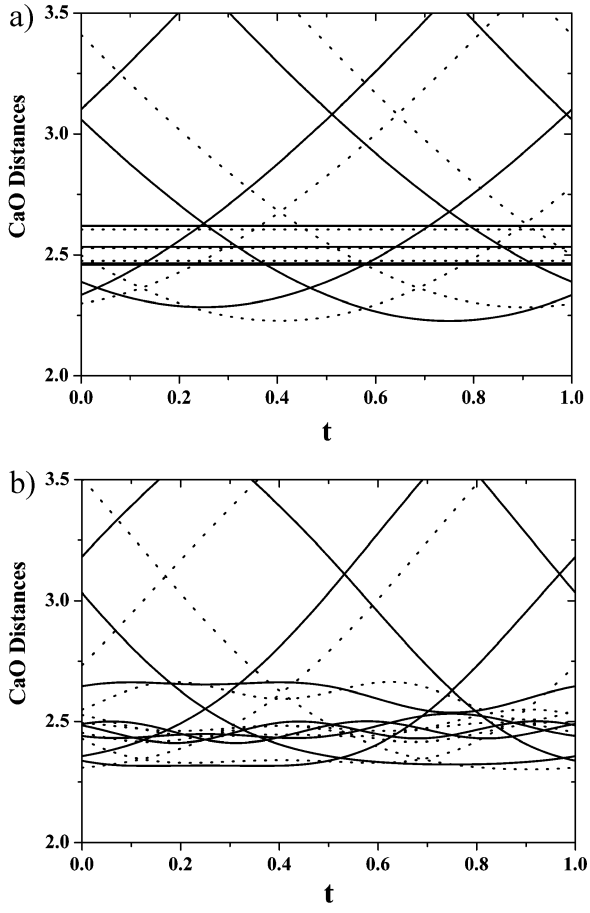

Figure 4. CaO interatomic distances: (a) without modulated displacements; (b) with modulated displacements. Ca1 solid lines; Ca2 dotted lines

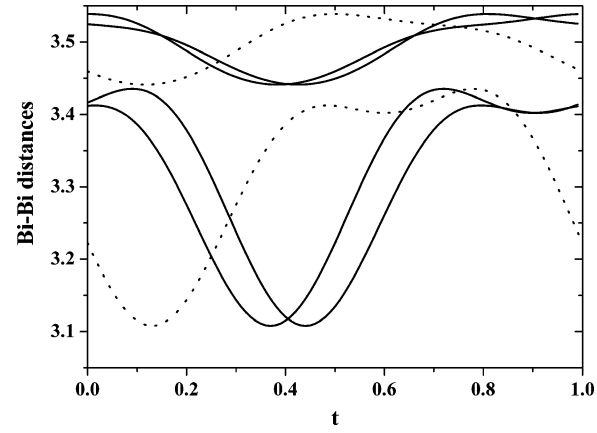

Figure 5. Bi−Bi distances as a function of *t*: (solid lines) Bi1−Bi distances; (dotted lines) Bi2−Bi distances. The shorter distances with large variations correspond to Bi−Bi distances within one double BiO chain.

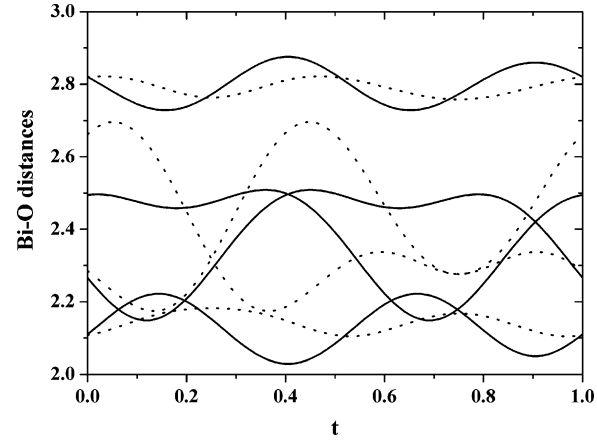

Figure 6. BiO distances as a function of *t*: (solid lines) Bi1−O; (dotted lines) Bi2−O. The shorter and longer BiO distances correspond to transverse bonds and show the double chain configuration. Intermediate ones with larger variations correspond to longitudinal ones.

modulated displacements prevent too short Ca−O distances to occur between the two subsystems, but allow to keep practically constant Ca−O distances close to 2.3 Å (Figure 4), with the Ca atom systematically bound to 2 or 3 oxygen atoms of the CoO_2 layer (Figure 3).

The second contribution can be interpreted as a mainly longitudinal modulation of the BiO layer, which results in the alternation within one double chain of domains with rather short Bi−Bi distances (compressed domains) with domains with larger Bi−Bi distances (extended domains) (Figure 5). The BiO distances (Figure 6) show the same phenomenon: transverse Bi−O distances have rather small variations but longitudinal Bi−O distances show the same alternation as the Bi−Bi distances, with smaller compressed domains (Bi−Bi 3.1–3.2 Å, Bi−O 2.2–2.3 Å) than extended domains (Bi−Bi 3.4 Å; Bi−O 2.5 Å). This type of modulation is very characteristic of these Bi−O layers in all modulated lamellar structures.[31–33] It reveals an adaptability of these layers which allows the corresponding structures to accommodate a lattice mismatch between different stacked layers. As a matter of fact, the a parameter is a common parameter between the two subsystems of the misfit structure and so is also common with the BSCO structure. It corresponds to the pseudohexagonal CoO_2 structure with a O−O distance of 2.8 Å (4.9 Å $\approx 2.8 \times \sqrt{3}$) and to the parameter of the rocksalt system (around two Bi−O distances). The substitution of Ca for Sr cannot modify this parameter which is fixed by the rigid pseudohexagonal CoO_2 layer. Such a constraint does not exist in the two other directions (misfit direction with the corresponding flexibility of the aperiodic structure and stacking direction of these lamellar structures) and we observe a significant reduction of the corresponding b and c parameters for BCCO compared with BSCO (4.7 vs 5.2 Å, and 29.33 vs 29.86 Å). The BiO layers sandwiched between the CaO or SrO layers are systematically extended layers when considering usual Bi−O distances. The stability of the corresponding chains is probably higher when aligned with the smaller available in plane cell parameter ($a = 4.9$ Å for BSCO and $b = 4.7$ Å for BCCO). This explains the difference of orientation of the modulation in both structures (Figure 2) and why in BCCO, the modulation can lock on the same aperiodicity than the misfit, using the $\mathbf{q}_2^*$ vector (*x*-component of 0.309 vs 0.293 for BSCO).

Another significant common point with the BSCO structure is the refinement of significant modulation waves for the occupation of the Bi site. A very similar modulation was observed in the BSCO structure. It shows the existence of vacancies in the compressed domains. They are also correlated with a large increase of the u_{22} modulated ADP parameters (Figure 7). The corresponding parameters are

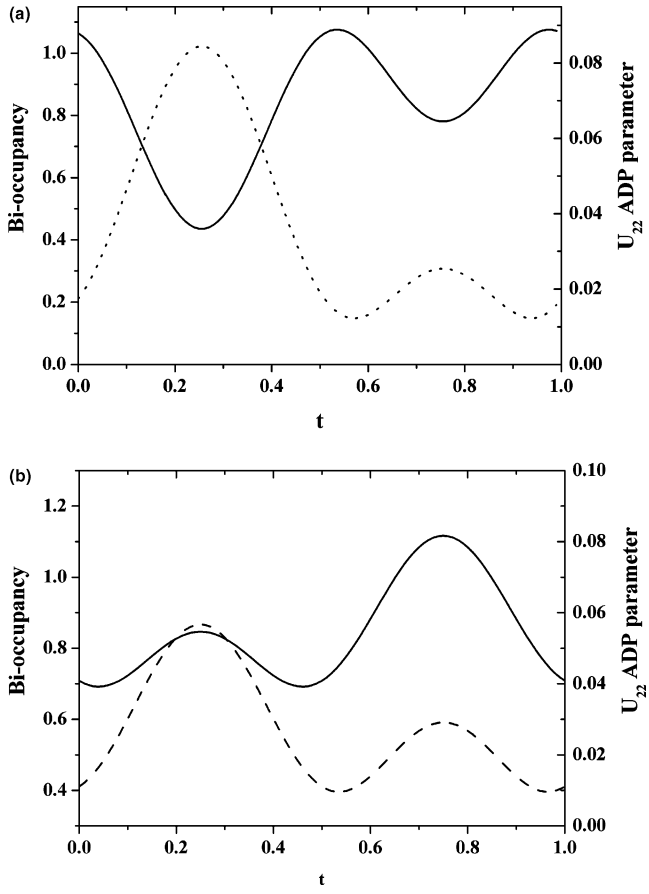

Figure 7. Bi site occupancy (solid lines) and u_{22} ADP parameter (dotted lines) as a function of *t*. (a) Bi1. (b) Bi2.

probably correlated and could be explained by a static disorder in the Bi position as it was observed for the Bi based high T_c superconducting copper oxides. The refined value for the average occupancy of the Bi site is smaller than the value obtained by EDS analysis. This can be explained first by residual Bi oxide on the surface of the sample resulting from the synthesis conditions (Bi_2O_3 residues were found in the preparation), and second by the harmonic model for the modulation parameters which is not sufficient for a valuable estimation of the variations of this occupation in the different parts of the Bi−O chains, in relation also with the large ADP parameters.

5. Conclusion

The substitution of Sr for Ca in the four layer lamellar misfit cobalt oxides leads in the same time to very large similarities, but also to significant differences. The general misfit structure is preserved, with new cell parameters and misfit ratio in relation with the smaller Ca atom. The misfit system is stabilized by displacive Ca and O modulations allowing a robust bonding scheme between both subsystems in the same way as for BSCO. Double Bi−O chains are clearly still present, but with a new orientation corresponding to the misfit aperiodic direction. As these Bi−O chains are known to show very frequently specific displacive modulations, this is still confirmed and proved here that this versatility is a tool to accommodate the cell parameter mismatch. This specific modulation is here characterized by the same irrational part of the modulation vector as in the misfit structure, so that both types of satellite reflections can be indexed in the same manner. The structure can formally be described in a 4D description but still be interpreted with two specific origins of modulation. The main characteristics of the intrinsic modulation of the Bi−O layer are still observed here, even concerning the Bi occupation modulation. Nevertheless, the lower values of the Bi occupancy function can also be explained by a likely disorder on this site. So, it was possible here to describe in the framework of only one incommensurate modulation, two different chemical and structural independent phenomena, which can in this specific case accommodate the same aperiodic wavelength and orientation.

The CoO_2 layer is very similar to all the other corresponding layers in all these related thermoelectric Co oxide compounds. This is particularly remarkable because they are described in very different symmetries, which are all pseudosymmetries of the same hexagonal one, for this layer, but which differ according to the first rocksalt type subsystem. The thermoelectric power measured for these compounds are significantly different and in particular directly related to the misfit ratio. We confirm here that the substitution of Ca for Sr leads to an improvement of the thermoelectric power.[34] This misfit ratio induces different dopings of the CoO_2 layer, but one has also to take into account cation or anion vacancies, or the structural aspect of the rocksalt block, which can also highly influence this doping and the corresponding Co valence. The four layers block is here more favorable than the three layers one of CCO. Clearly, for the same misfit ratio, the structure, the microstructure and degree of order of this block has to be accounted for. This is still more important when we consider the associated properties relevant to the figure of merit, i.e. electrical and thermal conductivities. A clear conclusion of the present comparison is that these different dopings have apparently a negligible influence on the structural characteristics of the CoO_2 layers and of the corresponding distorted octahedra. The corresponding distortion (8% compression along *z*, 6 equal Co−O distances, a mutual slight shift of the two O layers, with the loss of the corresponding global ternary symmetry) is a main characteristic for a good thermoelectric behavior and has to be taken into account for a proper simulation of electronic properties. It seems in particular related to the low spin configuration of the Co atoms in this slice. But it is not sufficient by itself for an optimization of the physical properties.

Acknowledgment. The authors thank Hélène Rousselière for technical assistance and X-ray diffraction data collection.

IC701717F

(34) Maignan, A.; Hébert, S.; Pelloquin, D.; Michel, C. *J. Appl. Phys.* **2002**, *92*, 1964.